Effect of Coefficient of Thermal Expansion on Positive Temperature Coefficient of Resistivity Behavior of HDPE–Cu Composites

Prativa Kar, B. B. Khatua

Materials Science Center, Indian Institute of Technology, Kharagpur 721 302, India

Received 22 September 2009; accepted 14 March 2010
DOI 10.1002/app.32455
Published online 27 May 2010 in Wiley InterScience (www.interscience.wiley.com).

ABSTRACT: Positive temperature coefficient of resistivity (PTCR) characteristics of (high density polyethylene) HDPE–Cu composites has been investigated with reference to the conventional HDPE–CB (carbon black) composites. Plot of resistivity against temperature of HDPE–CB composites showed a sudden rise in resistivity (PTC trip) at 127°C, close to the melting temperature of HDPE. However, the PTC trip temperature (98°C) for HDPE–Cu composites was appeared well below the melting temperature of HDPE. Addition of 1 phr nanoclay in the composites resulted in an increase in PTC trip temperature of HDPE–Cu composites, whereas no significant effect of nanoclay on PTC trip temperature was evident in case of HDPE–CB–clay composites. We proposed that the PTC trip temperature in HDPE–Cu composites was governed by the difference in coefficient of thermal expansion (CTE) of HDPE and Cu. The room temperature resistivity and PTC trip temperature of HDPE–Cu composites were very much stable upon thermal cycling. DMA results showed higher storage modulus of HDPE–Cu composites than the HDPE–CB composites. Thermal stability of HDPE–Cu composites was also improved compared to that of HDPE–CB composites. © 2010 Wiley Periodicals, Inc. J Appl Polym Sci 118: 950–959, 2010

Key words: resistivity; PTCR; composites; CTE; clay

INTRODUCTION

Positive temperature coefficient to resistivity (PTCR) is an interesting phenomenon in the field of conducting polymer composites consisting of an insulating polymer matrix and conducting fillers. At room temperature the resistance of the material is very low. In the case of an over current situation, resistance rises within the positive temperature coefficient (PTC) region. This additional resistance in the circuit has the effect of reducing the overall current. Once the over current situation has been removed, internal temperature the PTC material drops resulting the resistance back to a low state.[1–7]

Since the discovery of PTCR effect in (low density polyethylene) LDPE–carbon black (CB) composite by Frydman,[1] many people have investigated the PTCR effect in different semicrystalline polymers filled with CB.[2–11] However, a great disadvantage associated with a sharp negative temperature coefficient (NTC) effect in CB filled semicrystalline polymer composites limits their application in over-temperature protections.[12] Crosslinking of the semicrystalline polymer matrix by peroxide, gamma radiation, or electron beam has been reported to eliminate the NTC effect.[13,14] Chan et al.[15,16] have reported that presence of very high molecular weight PE in (UHMWPE–CB) and (UHMWPE–PP–CB) composites could eliminate the NTC effect even though they were not crosslinked. Feng and Chan[17] observed a double PTC effect in ethylene tetrafluoroethylene (ETFE)–HDPE–CB composite due to the consecutive melting of HDPE and ETFE. Zhang and Pan[18] reported that surface treatment of Sn–Pb alloy with titanate agent improved the double PTC effect of Sn–Pb–HDPE composite. Park et al.[19] showed that the thermal expansion of polymer matrix near the crystalline melting temperature increased the resistivity of different thermoplastic polymers (EVA, LDPE, LLDPE and PP)–CB composites. Horibe et al.[20,21] reported increase in room temperature resistivity of HDPE–CB (55 wt %) composites with increasing the crystallinity of HDPE, CB content and decreasing CB particle size. They showed that HDPE–tungsten (41 vol %) composites had a lower room temperature resistivity and higher PTC intensity than that of HDPE–CB. However, in both the composites PTC trip was appeared only after the melting of HDPE. Shen et al.[22,23] have reported that the thermal volume expansion in HDPE–CB and PS–CB composites was the key factors responsible for increase in resistivity for the PTC effect. Zhou

Correspondence to: B. B. Khatua (khatuabb@matsc.iitkgp.ernet.in).

et al.[24] showed that in HDPE–CB composites the resistance changes at lower temperatures and in melting state were mainly attributed to the deformation of the polymer matrix, and elastic deformation of the CB network, respectively. Lee et al.[25] reported improvement in PTC intensity and repeatability of HDPE–CB composite in presence of small amount of multiwalled carbon nanotube (MWNT). Kalappa et al.[26] reported a significant volume expansion and noticeable PTCR effect in polyaniline (PANI)–MWNT–CB–HDPE hybrid nanocomposites near the melting point of HDPE. Li et al.[27] have reported a significant decrease in room temperature resistivity and improvement of PTC intensity of HDPE–CB composites in presence of graphite nanofibers.

In summary, literature on PTCR polymer composites reports that PTCR trip temperature is a function of melting temperature of the matrix polymer, and depends on polymer-filler combinations. Thus, the loss in dimensional stability of polymer matrix near the melting temperature is a major concern that leads to the disadvantage of PTCR polymer composites. Although, different theories have been proposed[28,29] to explain the PTCR behavior, the actual principle by which the polymeric PTCR composites provide overcurrent circuit protection is less clear and required further discussion. Different conducting fillers used in polymeric PTCR composites include nonmetallic (CB) and metallic powders such as, tin, gold, and silver.[30] Alternatively, ceramic powders, such as tungsten carbide,[31] vanadium oxide, (V_2O_5),[32,33] also have been used in PTCR composites. However, these fillers are expensive and thus needs to develop less expensive polymeric PTCR composites. PTCR composites show poor reproducibility of resistivity during a long period of time or when undergoing thermal cycles.[34] The objective of our work is to develop PTCR polymer composites with PTC trip temperature well below the melting temperature of polymer matrix. Thus, we prepared HDPE–Copper (Cu) powder composites by conventional melt processing method. The reason behind choosing HDPE and Cu was that HDPE has very high value of coefficient of thermal expansion (CTE) than that of Cu. We found that, the PTC trip temperature of HDPE–Cu composites appeared well below the melting temperature of HDPE. A plausible mechanism behind the PTCR effect in HDPE–Cu composites has been proposed with reference to the HDPE–CB composites. Here, we focus on the details of our findings.

EXPERIMENTAL

Materials used

HDPE used in this study was of commercial grade (M5018L) and procured from Haldia Petrochemicals, Haldia, India. Commercial grade (Ketjenblack EC-300J, average particle size: 30 nm) conducting carbon black (CB) was supplied by Akzo Nobel Chemicals, IL. The organoclay used in this study was Cloisite 20A (Southern Clay Product, TX). It is a montmorillonite modified with dimethyl dihydrogenated tallow ammonium to increase the domain (d) spacing of Na^+-montmorillonite. The cation exchange capacity of Cloisite 20A is 95 mequiv/100g. Hereafter, Cloisite 20A is referred to as the clay. High purity electrolytic copper (Cu) powder used in this study was of electrical contact grade (average particle size of 75 μm) and obtained from Sarda Industrial Enterprises, Mumbai, India.

TABLE I
Compounding Formulations for HDPE–CB and HDPE–Cu Composites

HDPE	Carbon black (CB), (g)	Copper powder (Cu), (g)	Clay in polymer (phr)
90	10	0	0
90	10	0	1
70	0	30	0
70	0	30	1
60	0	40	0

Preparation of the composites

Composites of HDPE with CB and copper powder were prepared by conventional melt blending in an internal mixture (Brabender Plasticorder) at 160°C, with a rotor speed of 40 rpm for 15 min. The compounding formulation for the composites is shown in Table I. Prior to the melt mixing, all the ingredients (HDPE, CB, clay, copper powder) were kept in air oven at 80°C to avoid any moisture indiced thermal degradation during mixing. All the ingredients in the composites formulation were then dry mixed and fed into the internal mixer at 160°C for melt mixing. Finally, the composites were compression molded at 160°C into different shapes for further characterizations.

CHARACTERIZATION

Measurement of PTCR characteristics

Compression molded impact bar samples were cryogenic fractured along the length at two ends. Hole with diameter of 1.5 mm and depth of $\sim$ 3 mm on center of sample along the thickness was made on each sample and a thermocouple was inserted to measure the actual sample temperature. Silver paint was applied to the fractured surfaces and dried at room temperature for 10 h. The sample was clamped with electrodes and with increasing temperature through uniform heating inside the oven, resistance

was measured with a multimeter and temperature was recorded across the sample with temperature indicator. The ambient temperature was controlled using the oven with an accuracy of ±0.5°C. This process of measuring PTC characteristics is referred to as static measurement technique.

Alternative current (AC) and direct current (DC) voltage adjusted by a voltage controller was applied on the sample along the length direction and the current passing through the sample was recorded using a digital multimeter. The heating behavior was characterized by measuring the surface temperature as a function of voltage and time. After the current and the surface temperature reached their steady values, the voltage was switched off and the sample was naturally cooled down to the room temperature. A higher voltage was then applied on the sample and the same measurement procedure was carried out. This process of measuring PTC characteristics is referred to as dynamic measurement technique.

TMA analysis

Linear changes in sample dimension (CTE) as a function of temperature of the pure HDPE and its composites were investigated through thermo mechanical analyzer (TMA, Perkin Elmer). The measurement was carried out with the sample having length of 2.2 mm and cross section area of 5.3 mm^2. The sample was scanned under nitrogen atmosphere from room temperature to 200°C at a heating rate of 5°C/min.

DSC study

The transition temperature (T_m) of HDPE and its composites were determined with differential scanning calorimetry (DSC-200 PC, NETZSCH) with a heating rate of 10°C/min, under nitrogen atmosphere. The samples were heated from room temperature to 175°C, and then cooled to room temperature at a cooling rate of 10°C/min. The second heating scans were taken for determination of melting temperature of the sample.

SEM study

The scanning electron microscope (SEM, VEGA II LSU, TESCAN, Czech Republic) was used to study the morphology of the composites. The specimens were carefully broken at liquid nitrogen atmosphere. Then the fracture surface of the samples was coated with a thin layer of gold to prevent charging. SEM micrographs were taken at an operating voltage of 5 kv.

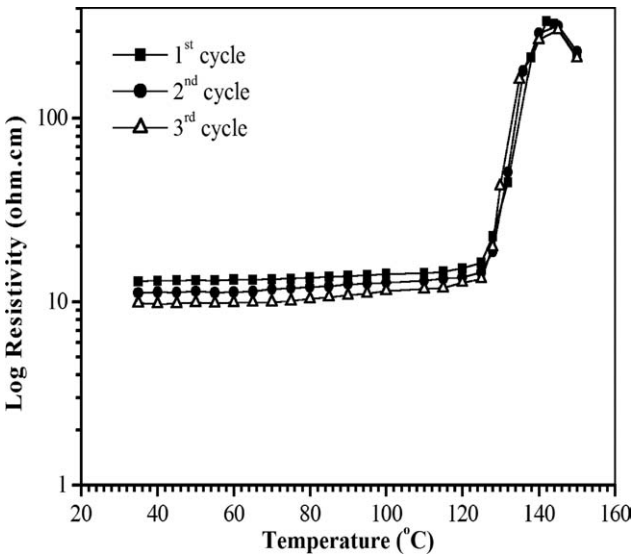

Figure 1 Resistivity temperature curves of HDPE–CB (10 wt %) composites at three consecutive heating cycle.

DMA analysis

Dynamic modulus of the composites was measured by a dynamic mechanical analyzer (DMA 2980 model). The dynamic temperature spectra of the composites were obtained in tension film mode at a constant vibration frequency of 1 Hz, temperature range of 30–150°C at a heating rate of 5°C/min, in nitrogen atmosphere. The dimension of the specimen was 30 × 6.40 × 0.45 mm^3.

TGA analysis

The thermal stability (onset degradation temperature and temperature corresponds to 50 wt % loss and maximum wt loss) of the composites was investigated with the help of thermo gravimetric analysis (TGA-209F, from NETZSCH). The sample was heated from room temperature to 600°C at a heating rate of 10°C/min, under air atmosphere.

RESULTS AND DISCUSSION

Temperature resistivity study under static measurement

Figure 1 represents the variation of resistivity with temperature for the HDPE–CB (10 wt %) composites at different heating cycles. As observed, room temperature resistivity of the HDPE–CB composites did not show any remarkable changes up to 125°C. However, a sudden increase in resistivity of the composite was prominent at ~ 128°C. For instance, room temperature resistivity (13.0 ohm cm) of the composites was increased to 44.8 ohm cm at 128°C. This indicated that HDPE–CB composite showed the PTC trip temperature at ~ 128°C which was close to

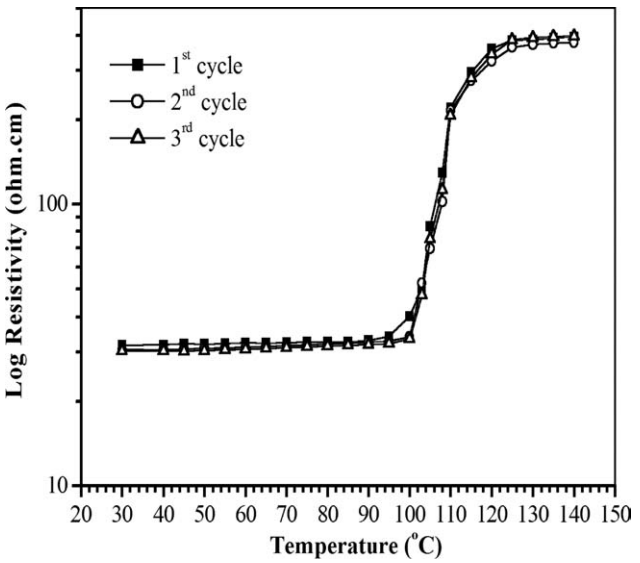

Figure 2 Resistivity temperature curves of HDPE–Cu (30 wt %) composites at three consecutive heating cycle.

the melting temperature of HDPE (onset of melting for HDPE starts at 129°C), consistent with the previous works.[35] The composites also showed a decrease in resistivity (NTC effect) at temperature above 140°C. This observation led us to conclude that the PTC trip temperature of the composites was governed by the melting of HDPE. At the melting temperature of HDPE, the disruption of continuous network structure of CB particles resulted in an increase in resistivity that made the composites insulating in nature. Again, room temperature resistivity of HDPE–CB composites was not stable upon thermal cycling, and kept on decreasing with the cycle time. However, the PTC trip of the composites did not change with cycling, indicating the trip temperature governed by the T_m of HDPE.

Interestingly, the PTCR characteristic of the HDPE composites filled with Cu powder showed the shifting of PTC trip to lower temperature region. Figure 2 represents the change in resistivity of HDPE–Cu powder (30 wt %) composites with temperature. As observed, the room temperature resistivity (31.7 ohm cm) of HDPE–Cu powder composites was higher than that of HDPE–CB composites. However, in contrast to HDPE–CB system, the Cu powder filled composites showed a significant increase in resistivity ($\sim$ 40.3 ohm cm) at a lower temperature of $\sim$ 98°C. Thus the PTCR trip temperature of HDPE–Cu powder composites was well below the trip temperature of HDPE–CB composites, and melting temperature of HDPE. This indicated that the PTCR phenomena in HDPE–Cu powder composites was not in agreement with the mechanism of crystalline PTCR effect in semicrystalline polymers composites with CB that showed the PTC trip temperature near the melting point of the matrix polymer (HDPE–CB system as shown in Fig. 1). Thus, the PTC trip temperature ($\sim$ 98°C) for HDPE–Cu powder system indicated that the mechanism behind the PTC trip temperatures of the composites was different, when compared to the PTCR mechanism of HDPE–CB composite system. Again, room temperature resistivity of HDPE–Cu composites did not show any remarkable change with thermal cycling. As the trip temperature of the composites was well below the T_m of HDPE, Cu particles could not move in the solid HDPE matrix at trip temperature. Thus, formation of same continuous network of Cu particles might be possible after cooling the composites to room temperature.

To explain the observed PTCR trip temperatures in HDPE–Cu composites, we considered the CTE values of HDPE and Cu powder. It is well known that the CTE value of polymer (except heat shrinkable polymers) is higher than metallic and ceramic particles. The CTE of HDPE ($\sim$ 200 ppm/°C) is remarkably higher than that of the Cu powder (17 ppm/°C).[36] Thus, in electrically conducting HDPE–Cu (30 wt %) composite, the Cu particles formed a continuous network structure in HDPE matrix. As the metal filler (Cu) had lower CTE value, when compared to the matrix polymer (HDPE), with increasing temperature the difference between the CTE values of filler and polymer at certain temperature resulted in a disconnection (local phenomena) of filler–filler particles in the network structure. This disruption in filler–filler particle contact led to a sudden rise in electrical resistivity. Thus, considering the filler-polymer CTE mismatch effect, a plausible mechanistic pathway behind the PTCR phenomena for HDPE–Cu system at a particular temperature (PTC trip temperature) when volume expansion of HDPE is enough to disconnect the filler–filler particles has been illustrated in Figure 3.

If the above assumption for the role of CTE mismatch on PTCR effect is true, then one can expect increase in PTC trip temperature of the HDPE–Cu powder composites having relatively lower CTE of the HDPsE matrix. To check this possibility we

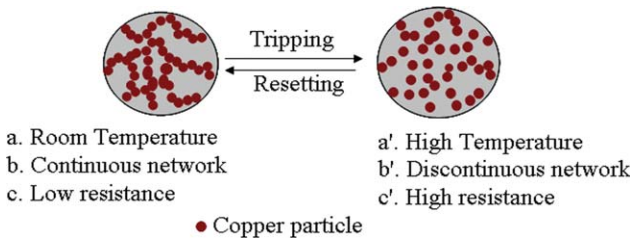

Figure 3 Schematic representation for the PTCR effect in HDPE–Cu composites. [Color figure can be viewed in the online issue, which is available at www.interscience.wiley.com.]

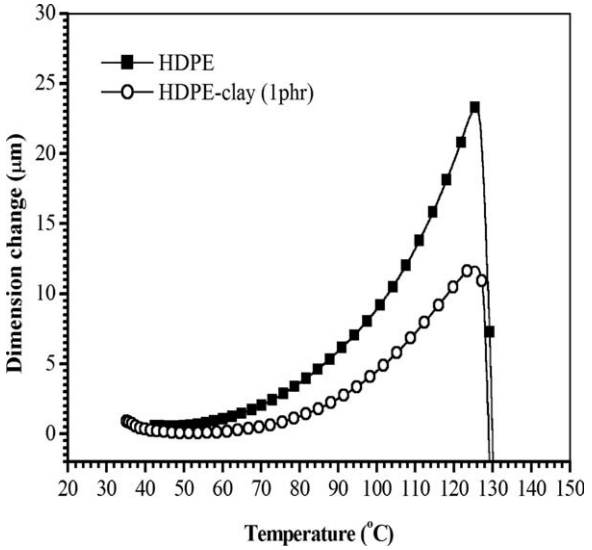

Figure 4 TMA plots showing the change in volume with temperature for HDPE and HDPE–clay (1 phr) nanocomposites.

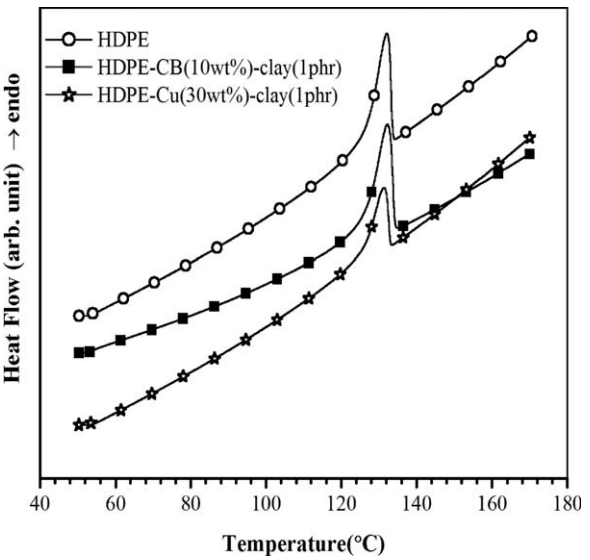

Figure 5 DSC thermograms of pure HDPE, HDPE–CB–clay, and HDPE–Cu–clay composites. The amount of clay in all the composites were 1 phr with respect to HDPE.

studied the PTCR characteristics of (HDPE–clay)–Cu powder (30 wt %) composites. Addition of nanoclay is known to decrease the CTE of polymers in the nanocomposites.[37] Figure 4 represents the TMA plots of pure HDPE and its composites with 1 phr clay. As observed at certain temperature the CTE value of pure HDPE was considerably higher than that of HDPE–clay (1 phr) nanocomposites. This indicates that for similar volume expansion the nanocomposites will require relatively higher temperature than that of the neat polymer. The high CTE value of polymers is caused by the low energy barrier for the chain conformation to be changed. The decrease in CTE value of the polymer in intercalated/exfoliated polymer–clay nanocomposites is due to the confinement of polymer chains inside the clay galleries. In our previous work, we have shown that HDPE intercalates into the clay silicate layers.[38] We assume that, the high aspect ratio, stiff clay platelets act as barriers for the thermal diffusion process. Thus, the volumetric or linear thermal expansion coefficient of the polymer is reduced in the nanocomposites. We also checked the melting behavior of pure HDPE and that in the composites. Figure 5 represents the DSC heating scans of pure HDPE, HDPE–CB, and HDPE–Cu composites with 1 phr nanoclay. The DSC thermograms indicated that the temperature corresponding to the crystalline melting peak (T_m) of HDPE remain unaffected in both the composites.

Figure 6 shows the variation of resistivity with temperature for the HDPE–CB and HDPE–Cu powder (30 wt %) composites with and without clay (1 phr). As observed, addition of nanoclay had a marginal effect on the room temperature resistivity of the composites. For instance, composites of HDPE–CB with 1 phr of clay showed relatively lower room temperature resistivity (~ 11.3 ohm cm) compared to that without any clay (13.0 ohm cm). This might be due to better dispersion of CB particles in HDPE matrix in presence of clay. The increase in melt viscosity of HDPE in presence of clay helped to break down the CB clusters during melt blending, and prevented the agglomeration of CB particles leading to better dispersion. However, we did not observe any significant change in the PTCR characteristics of the HDPE–CB composites with and without 1 phr clay.

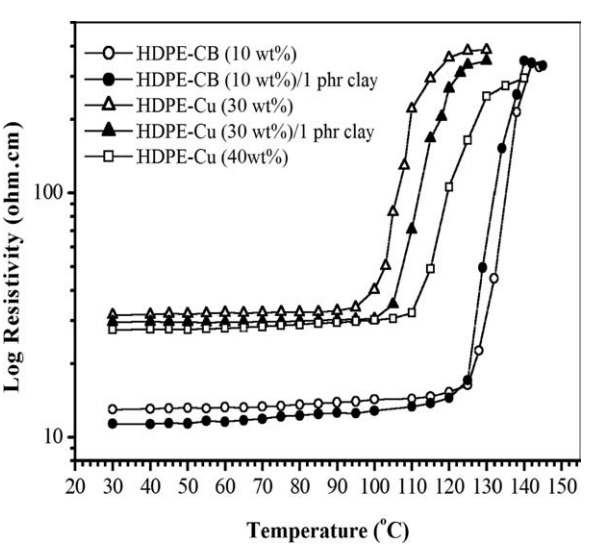

Figure 6 Resistivity temperature curves of HDPE–CB and HDPE–Cu composites without and with clay.

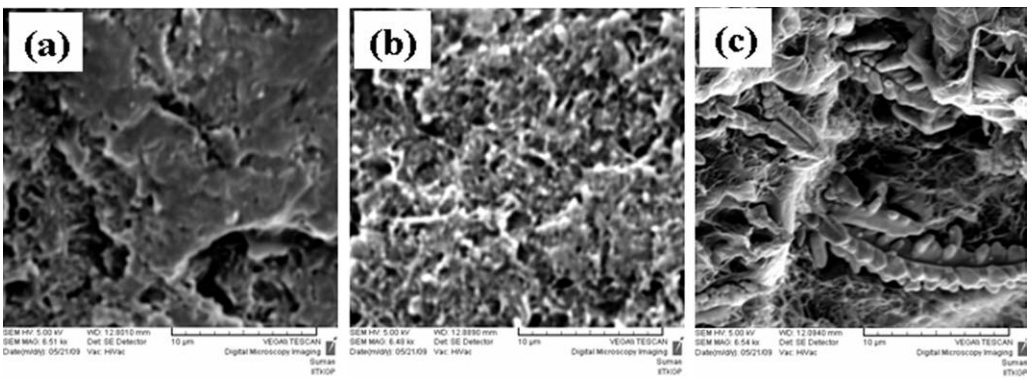

Figure 7 SEM images of the (a) HDPE–CB, (b) HDPE–CB–Clay, and (c) HDPE–Cu composites.

The PTCR trip of the HDPE–CB nanocomposites was appeared at ~ 128°C, similar to that of HDPE–CB composites system.

However, the PTCR trip temperature (~ 98°C) of the HDPE–Cu powder composites was shifted to ~ 105°C when the composites was formulated with 1 phr of clay (Fig. 6). It is interesting to note that the PTC trip temperatures of the HDPE–Cu powder composites with and without clay (1 phr) were very similar to the temperatures correspond to the same CTE values of HDPE and its nanocomposites with 1 phr of clay (Fig. 4). For instance, the extent of expansion of pure HDPE at ~ 95°C was comparable to that with HDPE–clay (1 phr) nanocomposites at ~ 107°C. This led us to conclude that the mismatch in CTE values of HDPE and Cu particles at ~ 98 and ~ 105°C were enough to break the continuous network structure of Cu particles in HDPE–Cu composites without and with 1 phr of clay, respectively.

We also investigated the PTCR characteristic of the HDPE–Cu composites with relatively higher loading level (40 wt %) of Cu powder (Fig. 6). The resistivity (27.6 ohm cm) of the composites was decreased when compared to that loaded with 30 wt % of Cu powder. This was due to the formation of more continuous network structure (Cu–Cu contact points) of Cu powders at higher loading that reduced the contact resistance. However, the PTCR trip temperature of the HDPE–Cu (40 wt %) composites was increased to ~ 112°C, which was much higher than that of HDPE–Cu (30 wt %) composites. The shifting of PTC trip temperature to higher temperature region at higher amount of Cu powder loading can be explained by considering the increased number of Cu–Cu contact points. Thus, the difference in CTE of HDPE and Cu powder at higher temperature (~ 112°C) could disrupt the continuous structure of the conducting pathways. These observations indicated that the difference in CTE between HDPE and Cu played an important role that governed the PTC trip temperature in HDPE–Cu composites.

Morphology study

One can comment on why HDPE–CB composites under investigation did not show the PTCR trip in the temperature region similar to that with HDPE–Cu composites. To clarify this, we consider the particle sizes of CB and Cu powder under investigation and their extent of dispersion in HDPE matrix. The average particle size (D) of CB used in this study was ~ 30 nm, which was significantly smaller than the particle size of Cu powder (~ 75 μm). Thus, even at 10 wt % CB loading, the number of CB particles and branching on the continuous network structure in HDPE–CB composites were expected to be considerably higher than that in HDPE–Cu (30 wt %) composites.

Figure 7 represents the SEM images of the HDPE–CB, HDPE–CB–Clay, and HDPE–Cu composites. As observed, CB particles were dispersed mostly as agglomerates with poor distribution in HDPE matrix [Fig. 7(a)]. It is clear from the SEM image [Fig. 7(b)] that the extent of CB distribution was better in presence of clay than that without any clay. CB particles were more uniformly dispersed in the matrix with minor cluster formation. This led to the formation of more CB–CB contact points in HDPE matrix and hence reduced the resistivity of HDPE–CB composites. In contrast to HDPE–CB composites, distribution of Cu particles was not uniform in HDPE–Cu composites [Fig. 7(c)]. This indicated the formation of considerably less branching in the continuous network structure of Cu particles, when compared to that in HDPE–CB composites. We proposed that the difference in CTE between HDPE and CB at a temperature below the T_m of HDPE was not enough to bring separation in the continuous network of CB particles in HDPE matrix. Thus, PTC trip of HDPE–

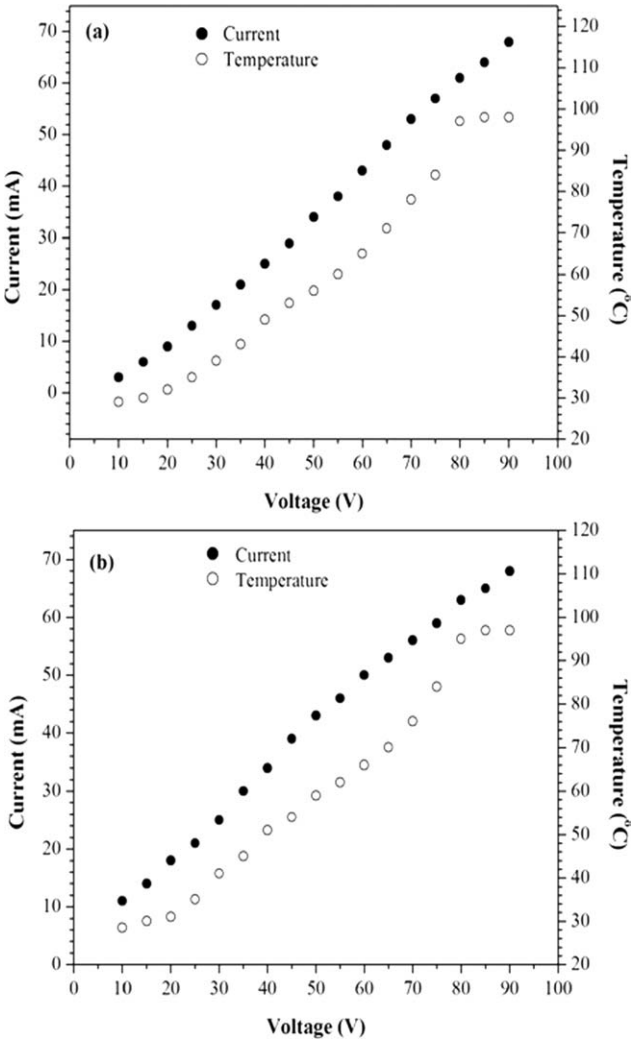

Figure 8 Current -Voltage (*I-V*) Characteristics of HDPE–Cu (30 wt %) composites under (a) AC Voltage and (b) DC voltage applications.

CB composites was appeared in the temperature region (T_m of HDPE) correspond to the maximum volume expansion of HDPE.

Studies on current-voltage (*I-V*) characteristics and PTCR effect under dynamic measurement

Figure 8 presents the current-voltage dependence for HDPE–Cu composites at 30 wt % Cu powder loading. It is clearly seen that at a high Cu loading of 30 wt % the conduction obey an Ohmic law. At room temperature, both under AC and DC applied voltages, the initial current (*I*) flow in the composites was increased with increasing the applied voltage. We also investigated the rise in maximum temperature in the composites at different AC and DC voltage applications. As observed, a maximum temperature of $\sim$ 97°C could be developed in the composites when the applied voltage (AC or DC) was increased to $\sim$ 80 volt. However, no further increase in temperature of the composites above this applied voltage clearly indicated that maximum temperature developed as a result of current flow was limited to the PTC trip temperature ($\sim$ 98°C) of the composites. This was due to sudden increase in resistance near PTC trip temperature that decreased the current flow in the composites.

The thermo-electric behavior of HDPE–Cu composites with time under 40 and 80 volt applications are shown in Figures 9 and 10, respectively. It is interesting to note that, the temperature of the composites was increased to a maximum of 53 and 55°C under 40V AC and DC applications [Fig. 9(a,b)], respectively. At 40 V application (AC and DC), *I* of the composites remain constant with time. This observation was also supported by the temperature resistivity measurement (Fig. 2) that indicated the room temperature resistivity of the composites

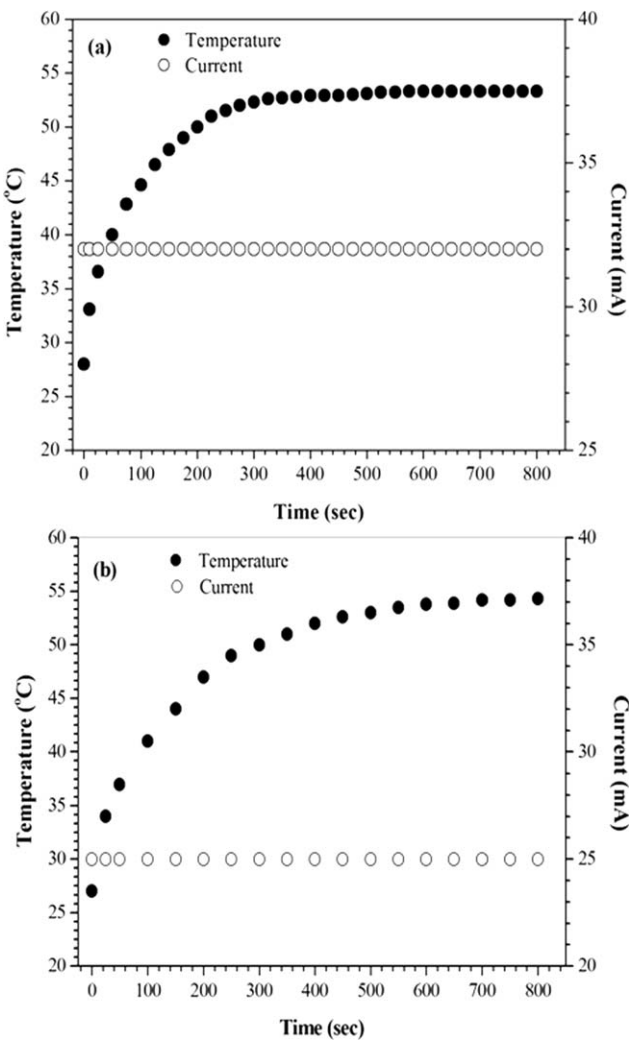

Figure 9 Temperature Current (*I*) plots of HDPE–Cu (30 wt %) composites under 40 V application: (a) AC voltage and (b) DC voltage.

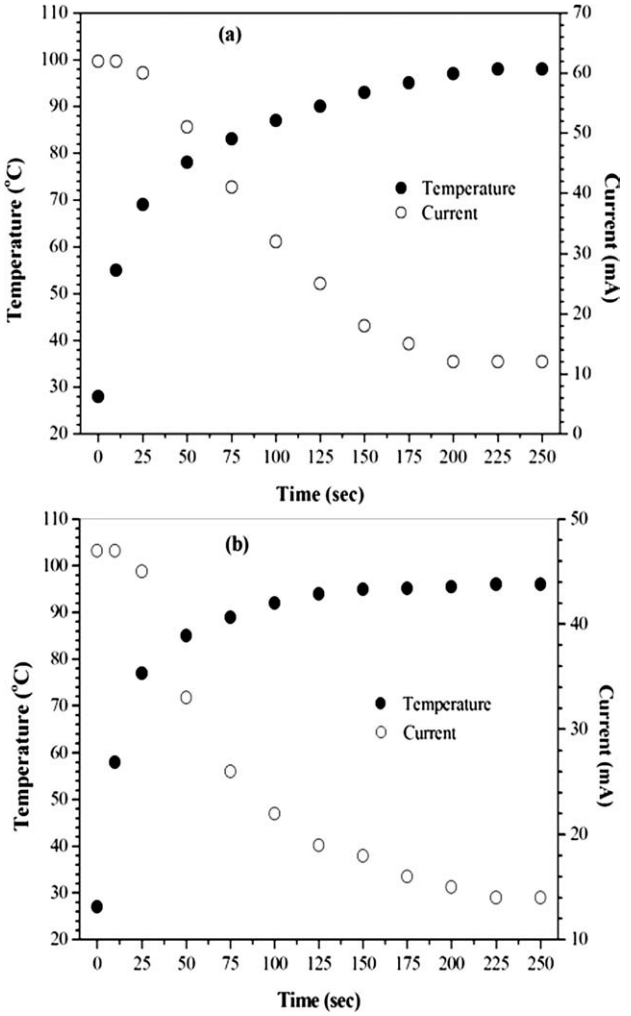

Figure 10 Temperature Current (*I*) plots of HDPE–Cu (30 wt %) composites under 80 V application: (a) AC voltage and (b) DC voltage.

remain constant at ~ 55°C. However, both under AC and DC applications, a sharp decrease in *I* was evident after 225 s when the applied voltage was increased to 80 V [Fig. 10(a,b)]. As observed, after 225 s under 80 V AC and DC application, the composites could attain 98°C and 96°C, respectively, which were close to the PTC trip temperature. Thus, increase in resistivity of the composites near the PTC trip temperature resulted in a decrease in *I* of the composites, and hence no further increase in temperature was observed.

Mechanical properties

Figure 11 represents the DMA plots of pure HDPE and its composites with CB and Cu powder. As observed, the storage modulus of HDPE was increased in both the composites throughout the entire temperature (25–125°C) scan. However, the improvement in storage modulus of HDPE was more prominent in HDPE–Cu composites, compared to the HDPE–CB composites. This may be due to higher loading of Cu powder in HDPE–Cu composites. It's noteworthy, the storage modulus of the composites at their respective PTCR trip temperatures revealed that HDPE–Cu composites had three times higher storage modulus than that of HDPE–CB composites. This observation clearly indicated that HDPE–Cu composites had remarkably high dimensional stability than the HDPE–CB composites at their PTCR trip temperatures.

Addition of small amount of nanoclay (1 phr) in HDPE–Cu composites led to further increase in storage modulus of the composites. The higher storage modulus of the composites in presence of clay is due to the reinforcing effect imparted by high aspect ratio clay platelets that allowed a greater degree of stress transfer at the interface. Again, restricted segmental motion of the intercalated polymer chains inside the clay galleries may be the possible cause for a phenomenal increase in the storage modulus.[39]

Thermo gravimetric analysis (TGA)

Figure 12 represents the TGA plot of pure HDPE, HDPE–CB, and HDPE–Cu composites without and with 1 phr clay. TGA analysis revealed that addition of CB and Cu powder increased the thermal stability of HDPE in the composites. This increase in thermal stability may arise from the interaction between the polymer chains and the fillers surfaces. It's also noteworthy that the increase in thermal stability was more in case of HDPE–Cu composites, when compared to that of HDPE–CB composites. The temperatures correspond to the initial degradation (T_1), 50% degradation (T_{50}), and maximum degradation (T_{max})

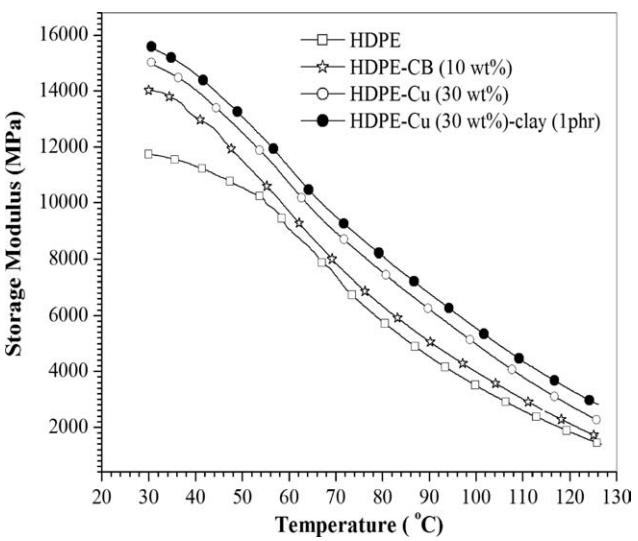

Figure 11 Storage modulus of pure HDPE, and its composites with CB (10 wt %) and Cu (30 wt %) powder, without and with clay.

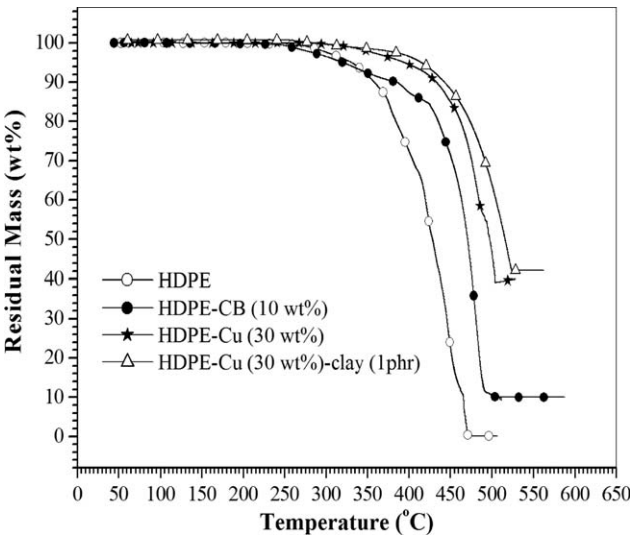

Figure 12 TGA thermograms of pure HDPE, HDPE–CB (10 wt %), and HDPE–Cu (30 wt %) composites without and with clay.

of the composites were calculated and shown in Table II. The initial degradation temperature (T_1) of pure HDPE remained almost unaffected in HDPE–CB composites. However, significant increase in T_1 was observed in HDPE–Cu composites. The temperatures corresponds to 50% weight loss (T_{50}) and maximum weight loss (T_{max}) of pure HDPE were shifted to higher temperature region in both the composites, with more significant increase in case of HDPE–Cu composites. Furthermore, addition of clay (1 phr) significantly increased the thermal stability of HDPE–Cu composites, when compared to that without any clay. The improvement in thermal stability of HDPE–Cu composite in presence of nanoclay is mainly due to the intercalation of HDPE into the clay galleries, which act as a barrier for thermal degradation. Nanoclay also acts as a superior insulator and mass transport barrier to the volatile products generated during decomposition which enhance thermal stability.[39] The high thermal stability of the HDPE–Cu composites, without or with clay, indicates that the composites can be efficiently used as PTCR material without any thermal degradation on cycling.

TABLE II
TGA Results of Pure HDPE, HDPE–CB, and HDPE–Cu Composites With and Without Clay

Sample details	T_1 (°C)	T_{50} (°C)	T_{max} (°C)
HDPE	283	429	472
HDPE–CB (10 wt %)	281	471	503
HDPE–Cu (30 wt %)	348	498	504
HDPE–Cu (30 wt %)–clay (1 phr)	359	514	525

CONCLUSIONS

In this study, we have shown the PTCR effect in conducting filler (Cu) filled HDPE composites. The PTCR trip temperature of HDPE–Cu (30 wt %) composites was observed well below the crystalline melting temperature (T_m) of matrix polymer. After thermal cycle, the composite exhibited almost the same room temperature resistivity and quite similar PTCR characteristics. Addition of small amount of nanoclay in the composites, that reduced the CTE of HDPE, shifted the PTCR trip temperature to higher temperature region. The same effect of nanoclay to PTCR trip temperature was not evident in HDPE–CB composites where tripping occurred near the T_m of HDPE. Thus, we proposed that the observed PTCR trip temperature in HDPE–Cu composites was a result of CTE mismatch between HDPE and Cu that could disrupt the continuous network structure of Cu particles in the composites well below the T_m of HDPE. The mechanical properties and thermal stability of the HDPE–Cu composites were also significantly higher than that of HDPE–CB composites. This result indicated that the HDPE–Cu composites could maintain their thermo sensitive and dimensional stability for a long time in a thermal environment in which the temperature was lower than melting temperature of HDPE.

Reference

1. Frydman, E. UK Pat Spec 6,041,95I,718-14S (1945).
2. Meyer, J. Polym Eng Sci 1973, 13, 462.
3. Meyer, J. Polym Eng Sci 1974, 14, 706.
4. Voet, A. Rubber Chem Technol 1981, 54, 42.
5. Klason, C.; Kubat, J. J Appl Polym Sci 1975, 19, 831.
6. Narkis, M.; Vaxman, A. J Appl Polym Sci 1984, 29, 1639.
7. Narkis, M.; Ram, A.; Stein, Z. J Appl Polym Sci 1980, 25, 1515.
8. Narkis, M.; Stein, Z.; Ram, A. Polym Eng Sci 1981, 21, 1049.
9. Narkis, M.; Ram, A.; Flashner, F. Polym Eng Sci 1978, 18, 649.
10. Feller, J. F.; Bruzaud, S.; Grohens, Y. Mater Lett 2004, 58, 739.
11. Mironi-Harpaz, I.; Narkis, M. Polym Eng Sci 2001, 41, 205.
12. Feng, J.; Chan, C.-M. Preprints of Second East Asian Polymer Conference; Hong Kong uni.sci.tech., Hong Kong, 1999; p 339.
13. Hou, Y. H.; Zhang, M. Q.; Rong, M. Z. J Polym Sci Part B: Polym Phys 2003, 41, 127.
14. Feller, F. J.; Linossier, I.; Levesque, G. Polym Adv Technol 2002, 13, 714.
15. Chan, C.-M.; Cheng, C.-L.; Yuen, M. M. F. Polym Eng Sci 1997, 37, 1127.
16. Feng, J.; Chan, C.-M. Polymer 2000, 41, 4559.
17. Feng, J.; Chan, C.-M. Polymer 2000, 41, 7279.
18. Zhang, X.; Pan, Y. Polym Int 2008, 57, 770.
19. Park, S.-J.; Kim, H.-C.; Kim, H.-Y. J Colloid Interface Sci 2002, 255, 145.
20. Horibe, H.; Kamimura, T.; Yoshida, K. Jpn J Appl Phys. I. Regul Pap Short Notes Rev Pap 2005, 44, 2025.
21. Horibe, H.; Kamimura, T.; Yoshida, K. Jpn J Appl Phys. I. Regul Pap Short Notes Rev Pap 2005, 44, 4171.
22. Shen, L.; Qian, Y. J.; Lou, Z. Fuhe Cailiao Xuebao/Acta Materiae Compositae Sinica 2008, 25, 13.

23. Shen, L.; Lou, Z. D.; Qian, Y. J. J Polym Sci Part B: Polym Phys 2007, 45, 3078.
24. Zhou, J.; Song, Y.; Shangguan, Y.; Zheng, Q. J Appl Polym Sci 2008, 110, 2001.
25. Lee, J.-H.; Kim, S. K.; Kim, N. H. Scr Mater 2006, 55, 1119.
26. Kalappa, P.; Lee, J.-H.; Rashmi, B. J.; Venkatesha, T. V.; Pai, K. V.; Xing, W. IEEE Trans Nanotechnol 2008, 7, 223.
27. Li, Q.; Siddaramaiah, B.; Kim, N. H.; Yoo, G.-H.; Lee, J. H. Compos B: Eng 2009, 40, 218.
28. Kohler, F. U.S. Pat. 3,243,753 (1966).
29. Ohe, K.; Naito, Y. Jpn J Appl Phys 1971, 10, 99.
30. Meyer, J. U.S. Pat. 3,673,121 (1972).
31. Tosaka, H.; Takaya, M.; Moriya, S.; Kobuke, H.; Hamada., M. U.S. Pat. 5,793,276 (1998).
32. Yi, X.; Wu, G.; Pan, Y. Polym Int 1997, 44, 117.
33. Wang, L.; Zhou, Z. IEEE Trans Compon Packag Manuf Technol Part A 1995, 18, 249.
34. Zhang, J. F.; Zheng, Q.; Yang, Y. Q.; Yi, X. S. J Appl Polym Sci 2002, 83, 3112.
35. Zhang, J. F.; Zheng, Q.; Yang, Y. Q.; Yi, X. S. J Appl Polym Sci 2002, 83, 3117.
36. Halahmi, I.; Erez, O.; Erez, A. U.S. Pat. 7,541,084 (2009).
37. Chen, B.; Liu, S.; Evans, J. R. G. J Appl Polym Sci 2008, 109, 1480.
38. Mallick, S.; Dhibar, A. K.; Khatua, B. B. J Appl Polym Sci 2010, 116, 1010.
39. Dhibar, A. K.; Mallick, S.; Rath, T.; Khatua, B. B. J Appl Polym Sci 2009, 113, 3012.